

Two-dimensional weak localization effects in high temperature superconductor



G. I. Harus, A. N. Ignatenkov, A. I. Ponomarev, L. D. Sabirzyanova, N. G. Shelushinina

Institute of Metal Physics

18 Kovalevskaya St., Ekaterinburg, 620219, Russia

A. A. Ivanov

Moscow Engineering Physics Institute, Moscow, 115409, Russia

A systematic study of the resistivity and Hall effect in single crystal $\text{Nd}_{2-x}\text{Ce}_x\text{CuO}_{4-\delta}$ films ($0.12 \leq x \leq 0.20$) is presented, with special emphasis on the low-temperature dependence of the normal state conductance. Two-dimensional weak localization effects are found both in a normally conducting underdoped sample ($x = 0.12$) and *in situ* superconducting optimally doped ($x = 0.15$) or overdoped ($x = 0.18$) samples in a high magnetic field $B > B_{c2}$. The phase coherence time τ_φ (5.4×10^{-11} s at 2K) and the effective thickness of a CuO_2 conducting layer d ($\cong 1.5\text{\AA}$) have been estimated by fitting 2D weak localization theory expressions to magnetoresistivity data for magnetic fields perpendicular to the *ab* plane and in plane. Estimates of the parameter d ensure strong carrier confinement and justify a model consisting of almost decoupled 2D metallic sheets for the $\text{Nd}_{2-x}\text{Ce}_x\text{CuO}_{4-\delta}$ single crystal.

PACS numbers: 74.60 Ec, 74.76 Bz.

I. INTRODUCTION

The field of high-transition-temperature (high- T_c) superconductivity has generated several thousand publications in the last few years. For a short overview of the lattice structure and phase diagram of the most widely studied copper oxide compounds, such as hole-doped $\text{La}_{2-x}\text{Sr}_x\text{CuO}_4$ and $\text{YBa}_2\text{Cu}_3\text{O}_{6+x}$ or electron-doped $\text{L}_{2-x}\text{Ce}_x\text{CuO}_4$ (L=Nd or Pr), one can consult, e.g., the review in Ref. [1] or book by Plakida [2]. The copper oxide high- T_c materials are basically tetragonal, and all of them have one or more CuO_2 planes in their structure, which are separated by layers of other atoms (Ba-O, La-O, Nd-O, ...). Most researchers empirically and theoretically have come to a consensus that superconductivity is related to processes occurring solely in the conducting CuO_2 planes, with the other layers simply providing the carriers (they are therefore called charge reservoirs). In the CuO_2 planes, each copper ion is strongly bonded to four oxygen ions separated by approximately 1.9 \AA .

Due to the layered character of the crystal structures, the high- T_c copper oxide compounds are highly anisotropic in their normal-state electrical properties. Although the resistivity in the CuO_2 planes, ρ_{ab} , shows metallic temperature dependence, the temperature behavior and the magnitude of the resistivity parallel to the *c* axis, ρ_c , are strongly dependent on crystal structure, and on the concentration of charge carriers.

Systematic data for ρ_c in a number of high- T_c materials obtained on well characterized single crystals are presented by Ito et al. [3]. For hole-doped systems $\text{YBa}_2\text{Cu}_3\text{O}_{6+x}$ and $\text{La}_{2-x}\text{Sr}_x\text{CuO}_4$ ρ_c exhibits a marked change in magnitude as well as in temperature dependence with changing hole concentration (i.e., changing x). For the underdoped (low x) and optimally doped (superconducting) compounds ρ_c is non-metallic ($d\rho_c/dT < 0$) at low enough temperatures. In both systems the anisotropy coefficient, ρ_c/ρ_{ab} , decreases noticeably with doping, being $\sim 10^2$ for the superconducting compounds.

The crystal structure T' of the electron doped $\text{Nd}_{2-x}\text{Ce}_x\text{CuO}_{4-\delta}$ system is the simplest among the superconducting cuprates with the perovskite structure [4]. The Cu atoms in the CuO_2 layers of hole-doped $\text{La}_{2-x}\text{Sr}_x\text{CuO}_4$ or $\text{Nd}_{2-x-y}\text{Ce}_x\text{Sr}_y\text{CuO}_{4-\delta}$ ($y > x$) superconductors are surrounded by apical O atoms, forming octahedrons (T structure) or semioctahedrons (T* structure). The most important difference in the crystal structures of $\text{Nd}_2(\text{Ce})\text{CuO}_4$ and $\text{La}_2(\text{Sr})\text{CuO}_4$ is that the apical oxygen atoms in the T' structure are displaced so as to make an isolated CuO_2 plane (Fig.1).

The undoped system Nd_2CuO_4 is an insulator, with the valence band mainly of O $2p$ character, and the empty conduction band being the upper Hubbard Cu $3d$ band. The Coulomb $3d - 3d$ repulsion at the Cu site U ($\cong 6 - 7$ eV) is strong, and it is greater than the oxygen to metal charge-transfer energy Δ ($\cong 1 - 2$ eV). As the gap between the conduction and valence bands is determined just by the energy Δ , these cuprates are classified as charge-transfer semiconductors [5].

The combination of Ce doping and O reduction results in *n*-type conduction in CuO_2 layers in $\text{Nd}_{2-x}\text{Ce}_x\text{CuO}_{4-\delta}$ single crystals [4,6]. An energy band structure calculation [7] shows that the Fermi level is located in a band of

$pd\sigma$ -type formed by $3d(x^2 - y^2)$ orbitals of Cu and $p_\sigma(x, y)$ orbitals of oxygen. The $pd\sigma$ band appears to be of highly two-dimensional (2D) character, with almost no dispersion in the z -direction normal to CuO_2 planes. The electrons are concentrated within the confines of conducting CuO_2 layers, separated from each other by a distance $c \cong 6\text{\AA}$.

In accordance with such a structure $\text{Nd}_{2-x}\text{Ce}_x\text{CuO}_{4-\delta}$, single crystals have a significantly higher resistive anisotropy than Y- or La- systems: $\rho_c/\rho_{ab} \cong 10^4$ for $x = 0.15$ [8,9] and for $x = 0.16 - 0.20$ with different values of oxygen deficiency δ [10] at room temperature, it increases with decreasing temperature [10]. Measurements by Ito et al. [3] for another electron-doped compound with the same T' structure, $\text{Pr}_{2-x}\text{Ce}_x\text{CuO}_{4-\delta}$, show that for $x = 0.15$ the anisotropy is very large, $\rho_c/\rho_{ab} \geq 10^4$, and non-metallic ρ_c is observed. Preliminary measurements on a Pr-system with different x indicated that, as in the case of Y- and La- systems, ρ_c decreases with increasing carrier concentration much more rapidly than ρ_{ab} .

The larger anisotropy in Nd- or Pr- systems compared with La- or Y- systems would imply that fluorite-type Nd_2O_2 or Pr_2O_2 layers block out-of-plane conduction more effectively than NaCl-type La_2O_2 or Ba_2O_2 layers [3].

The non-metallic behavior of out-of-plane conductance suggests that the carriers are confined tightly in the CuO_2 plane [3]. It is thus of interest to search for two-dimensional effects in the in-plane conductance of the layered cuprates. There are several previous reports on the manifestation of 2D weak localization effects in the in-plane conductance of $\text{Nd}_{2-x}\text{Ce}_x\text{CuO}_{4-\delta}$ single crystals or films. Thus a linear dependence of resistivity on $\ln T$ comes about at $T < T_c$ for samples with $x \cong 0.15$, in which the superconducting state is destroyed by a magnetic field [11]. Furthermore, a highly anisotropic negative magnetoresistance, predicted for 2D weak localization, has been observed in the nonsuperconducting state at low temperatures: in samples with $x = 0.11$ [12] and in unreduced samples with $x = 0.15$ [13] or $x = 0.18$ [14]. We report here a systematic study of 2D weak localization effects for a number of optimally reduced samples of $\text{Nd}_{2-x}\text{Ce}_x\text{CuO}_{4-\delta}$ with $0.12 \leq x \leq 0.20$.

II. EXPERIMENTAL PROCEDURE

The flux separation technique was used for $\text{Nd}_{2-x}\text{Ce}_x\text{CuO}_{4-\delta}$ film deposition [15]. High-quality c -axis oriented single crystal films with thickness around 5000\AA and $0.12 \leq x \leq 0.20$ were grown. The values of T_c after sample reduction are shown in Table 1.

Figure 2 demonstrates that T_c of the film with $x = 0.15$ is in agreement with previously published data for bulk single crystals [4]. The values of T_c for overdoped films with $x \geq 0.17$ are higher than for corresponding bulk crystals in accordance with the information of Xu *et al.* [16] that superconductivity survives up to $x = 0.22$ in $\text{Nd}_{2-x}\text{Ce}_x\text{CuO}_{4-\delta}$ films.

Standard four-terminal measurements of the resistivity ρ and Hall effect $R(\vec{j}||ab, \vec{B}||c)$ in the dc regime were carried out in the temperature range $T_c < T \leq 300\text{K}$ without a magnetic field B , and in magnetic fields up to $B = 12\text{T}$ at temperature down to 0.2K . The electrical contacts were prepared by evaporating thin silver strips onto the sample, and attaching silver wires to these with conducting glue.

III. RESULTS

The temperature dependence of the zero-field in-plane resistivity for the investigated samples at T up to 300K is shown in Fig. 3. A clear resistance minimum is observed at $T \cong 150\text{K}$ for the nonsuperconducting sample with $x = 0.12$. The $\rho(T)$ dependence is described by $\rho = \rho_0 + A \cdot T^2$ at $T = (20 - 180)\text{K}$ for $x = 0.15, 0.17,$ and 0.18 , and over the wider $T = (10 - 300)\text{K}$ for $x = 0.20$. The values of ρ_0 and A are presented in Table 1.

We describe here the magnetoresistance measurements only for the underdoped nonsuperconducting sample ($x = 0.12$) and for two overdoped superconducting samples ($x = 0.18$ and $x = 0.20$). Detailed investigations of $\rho(B, T)$ dependencies for the optimally doped sample with $x = 0.15$ were presented earlier [17], as were some results on the $x = 0.18$ sample [18].

In the superconducting samples, normal-state transport at low T is hidden unless the magnetic field stronger than the second critical field B_{c2} is applied. As we are interested in the low-temperature $\rho(T)$ dependence, we have destroyed the superconductivity with a magnetic field B_\perp perpendicular to the CuO_2 planes. In Fig. 4, the $\rho(B_\perp)$ dependence for $x = 0.20$ at $T = 1.3\text{K}$ and $T = 4.2\text{K}$ in a magnetic fields up to $B = 5.5\text{T}$ are presented. In the inset of Fig. 4, the dependence of the Hall coefficient R on magnetic field B_\perp at $T = 1.3\text{K}$ is also shown. On the assumption that $B_{c2}^\perp(T)$ is a field in which $\rho(B_\perp)$ and $R(B_\perp)$ at given T come up to their normal-state value, we have $B_{c2}^\perp = 2.2\text{T}$ at $T = 1.3\text{K}$ and $B_{c2}^\perp = 1.5\text{T}$ at $T = 4.2\text{K}$.

In our previous investigation [18] of the sample with $x = 0.18$, negative magnetoresistance was observed after the destruction of superconductivity by a magnetic field up to 5.5T at $T \geq 1.4\text{K}$. In Fig. 5 $\rho(B_\perp)$ is shown for this sample

at much lower temperatures (down to 0.2 K) and in fields up to 12 T. The inset of Fig. 5 shows an example of $R(B_{\perp})$ at given $T < T_c$. The nonmonotonic $R(B_{\perp})$ behavior, with reversal of the sign of the Hall effect, is usually observed in the mixed state of the superconductor [18,19]. The transition to the normal state is completed at $B = B_{c2}$, where the Hall coefficient becomes nearly constant with the same value as in the normal state at $T > T_c$ ($B_{c2} \cong 5$ T at $T = 0.2$ K). Values of B_{c2} for $x = 0.18$ estimated in this way at different temperatures are marked by the arrows in Fig. 6. This figure also clearly demonstrates the transition from positive to negative magnetoresistance after the suppression of superconductivity.

In Fig. 7, the results of the theoretical description of the magnetoconductivity at $B > B_{c2}$ are presented. Figure 8 demonstrates that the resistivity of the sample with $x = 0.18$ is a linear function of $\ln T$ in magnetic fields $B > B_{c2}$. The experimental points for $B = 1.5$ T are also shown. If the logarithmic temperature dependence of the resistivity is typical of the normal state, then the discrepancy between the experimental points and the logarithmic law indicates that the normal state has not yet been attained at $B = 1.5$ T.

We have also measured the in-plane conductivity in nonsuperconducting sample with $x = 0.12$ for magnetic fields perpendicular and parallel to the CuO_2 planes up to 5.5 T at $T = 1.9$ K and 4.2 K (Fig. 9). The positive magnetoconductivity (negative magnetoresistance) observed in this sample is obviously anisotropic relative to the direction of the magnetic field.

IV. DISCUSSION

A logarithmic temperature dependence of the conductivity is one indication of the interference quantum correction due to 2D weak localization. A magnetic field normal to the diffusion path of a carrier destroys the interference. In a two-dimensional system, it causes negative magnetoresistance for the field perpendicular to the plane, but no effect for the parallel configuration. Weak localization effects are almost totally suppressed for $B_{\perp} > B_{tr}$ [20], where the so called “transport field” is defined as the field at which

$$2\pi B_{tr}\ell^2 = \Phi_0. \quad (1)$$

Here ℓ is the elastic mean free path and $\Phi_0 = \pi\hbar/e$ is the elementary flux quantum.

Let us compare Eq. (1) with the relations between the coherence length ξ and the second critical field in the pure superconductor ($\xi \ll \ell$),

$$2\pi B_{c2}\xi^2 = \Phi_0, \quad (2)$$

or in the so-called “dirty limit” ($\xi \gg \ell$):

$$2\pi B_{c2}\xi\ell = \Phi_0. \quad (3)$$

From Eqs. (1) and (2) we have $B_{tr}/B_{c2} = (\xi/\ell)^2$, so $B_{tr} \ll B_{c2}$, and it is impossible to observe weak localization effects in the pure case. In contrast, from Eqs. (1) and (3) one has $B_{tr}/B_{c2} = (\xi/\ell)$, $B_{tr} > B_{c2}$, and weak localization should survive in the normal state ($B > B_{c2}$) of a dirty superconductor.

In Table 2, the parameters of investigated samples essential to a description of localization are presented. From the experimental values of the in-plane resistivity ρ and Hall constant R in the normal state, we have obtained the surface resistance $R_s = \rho/c$ per CuO_2 layer and the bulk and surface electron densities $n = (eR)^{-1}$ and $n_s = n \times c$ ($c = 6$ Å is the distance between CuO_2 layers). Using the relations [21] $\sigma_s = (e^2/\hbar)k_F\ell$ for the 2D conductance $\sigma_s = 1/R_s$, and $k_F = (2\pi n_s)^{1/2}$ for the Fermi wave vector, we have estimated the important parameter $k_F\ell$, the mean free path ℓ , and then according to Eq. (1) the characteristic field B_{tr} . For the sample with $x = 0.15$ we use the data of Ref. [17].

In a random two-dimensional system, the parameter $k_F\ell$ can serve as a measure of disorder [21]. It is seen from Table 2 that we have a wide range $\sim (1 - 10^2)$ of $k_F\ell$ in the investigated series of samples. For $k_F\ell \gg 1$, a true metallic conduction takes place in CuO_2 layer. Thus, we have a rather pure 2D system with $k_F\ell \sim 10$ for $x = 0.15$ or $x = 0.18$, and an extremely pure system with $k_F\ell \sim 10^2$ for $x = 0.20$. It is quite remarkable that even at such high values of the parameter $k_F\ell$, a trace of localization comes to light: for $B_{\perp} > B_{c2}$, ρ is greater at 1.3 K than at 4.2 K (see Fig. 4). As for the sample with $x = 0.12$, where $k_F\ell$ is of the order of unity, this system is in close proximity to transition from weak logarithmic to strong exponential localization as disorder increases ($k_F\ell$ decreases).

The second critical field B_{c2}^{\perp} at temperatures around $T \cong 1.4$ K (see Figs. 4 and 5) and values of ξ estimated according to Eqs. (2) or (3) are also shown in Table 2. In the pure system with $x = 0.20$, $\xi < \ell$, and negative magnetoresistance is not detected at $B > B_{c2}$, at least for $T \geq 1.3$ K (see Fig. 4). Systems with $x = 0.15$ and 0.18

are situated close to the dirty limit $\xi \gg \ell$, and there exist appreciable field ranges $B_{c2} < B < B_{tr}$ where negative magnetoresistance due to 2D weak localization is actually observed (see Ref. [17] and Fig. 6).

In 2D weak localization theory, the quantum correction to the Drude conductivity in a perpendicular magnetic field is [22]:

$$\Delta\sigma_s(B_\perp) = \alpha \frac{e^2}{2\pi^2\hbar} \left\{ \Psi\left(\frac{1}{2} + \frac{B_\varphi}{B_\perp}\right) - \Psi\left(\frac{1}{2} + \frac{B_{tr}}{B_\perp}\right) \right\} \quad (4)$$

where α is a factor of the order of unity, Ψ is the digamma function, and $B_\varphi = c\hbar/4eL_\varphi^2$. Here $L_\varphi = \sqrt{D\tau_\varphi}$ is the phase coherence length, D is the diffusion coefficient, and τ_φ is the phase breaking time.

The fit of (4) to the experimental $\sigma_s(B_\perp)$ data for $x = 0.18$ at $B_\perp > B_{c2}^\perp$ is shown in Fig. 7. For each temperature there are two fit parameters: the characteristic field B_φ (or L_φ) and the factor α . The widest range of requisite magnetic fields and thus the most accurate fit results are obtained for the lowest temperature $T = 0.2$ K. With $B_{tr} = 22.5$ T, the best fit is obtained for $B_\varphi \cong 0.1$ T ($L_\varphi = 560$ Å) and $\alpha = 6.6$. The fitting procedure is highly sensitive to the value of the parameter α . In contrast, the value of B_φ is obtained only to order of magnitude, as we have no zero-field and weak-field data. Nevertheless, there is no doubt that the inequality $B_\varphi \ll B_{tr}$ is valid.

In the field range $B_\varphi \ll B \ll B_{tr}$, the expression (4) can be written

$$\Delta\sigma_s(B_\perp) = \alpha \frac{e^2}{2\pi^2\hbar} \left\{ -\Psi\left(\frac{1}{2}\right) - \ln \frac{B_\perp}{B_{tr}} \right\}. \quad (5)$$

The inset of Fig. 7 shows that the experimental data at $T = 0.2$ K can be fitted rather closely by this simple formula over a wide range of fields, $5 \text{ T} \leq B \leq 11 \text{ T}$. But as we have the factor $\alpha = 6.6$, negative magnetoresistance is too large to be due to the destruction of weak localization only. Thus we conclude that some additional mechanism of negative magnetoresistance must be at work.

There exists another quantum correction to the normal-state conductivity with a logarithmic dependence of magnetoresistivity on B , namely the correction due to disorder-modified electron-electron interaction (EEI) in the Cooper channel [23]. In the range of magnetic fields $B_T \ll B \ll B_{tr}$, we have

$$\Delta\sigma_s^{EEI}(B_\perp) = -\frac{e^2}{2\pi^2\hbar} \cdot g(T) \cdot \ln\left(\frac{B_\perp}{B_{tr}}\right), \quad (6)$$

where $B_T = \pi c\hbar/2eL_T^2$, $L_T = \sqrt{\hbar D/kT}$ is the thermal coherence length, and $g(T)$ is the effective interaction constant of two electrons with opposite momenta. For the attractive electron-electron interaction due to virtual phonon exchange, $g > 0$, and according to (6) the magnetoresistance should be negative.

As we have dealt with *in situ* superconducting samples, so that $g > 0$, the contribution due to EEI is most probably the reason for the extra negative magnetoresistance at very low temperatures ($B_T = 0.02$ T at $T = 0.2$ K). With increasing temperature, the magnitude of the EEI contribution decreases rapidly ($\alpha = 2.5$ at $T = 0.8$ K), and at $T \geq 1$ K the estimated value of the factor is close to unity ($\alpha = 0.77$ at $T = 2.1$ K), as it should be for weak localization.

It should be noted that pronounced negative magnetoresistance due to the suppression of weak electron localization is observed in ordinary superconductors as well. The electron transport properties of three-dimensional (3D) amorphous α -Mo₃Si and α -Nb₃Ge superconducting films have been investigated in magnetic fields up to $B = 30$ T at temperatures down to $T = 0.35$ K [24]. The authors have found that both the temperature and field dependence of the resistivity ρ can be qualitatively described by weak localization theory. At low temperatures and in magnetic fields above the upper critical field, $B > B_{c2}$, magnetoconductivity is proportional to $B^{1/2}$. This field dependence is consistent with weak localization in the high-field limit ($B \gg B_\varphi$) for 3D disordered systems, in contrast to a 2D system with $\Delta\sigma(B) \sim \ln B$.

One important indication of the 2D character of a system is the strong dependence of magnetoresistance on magnetic field orientation. Highly anisotropic (negative) magnetoresistance is actually observed in a nonsuperconducting sample with $x = 0.12$ (see Fig. 9). From the fit to $\sigma_s(B_\perp)$ by the functional form (4) with $\alpha = 1$, we find $L_\varphi = 770$ Å at $T = 1.9$ K and $L_\varphi = 550$ Å at $T = 4.2$ K, so that the phase coherence time $\tau_\varphi = 5.4 \times 10^{-11}$ s at $T = 1.9$ K and $\tau_\varphi = 2.7 \times 10^{-11}$ s at $T = 4.2$ K.

We explain the much weaker negative magnetoresistance for the parallel configuration $B \parallel ab$ by incorporating finite-thickness (d) corrections into the strictly 2D theory [25]:

$$\Delta\sigma_s(B_\parallel) = \frac{e^2}{2\pi^2\hbar} \cdot \ln\left(1 + \frac{d^2 L_\varphi^2}{3\lambda_\parallel^4}\right), \quad \lambda_\parallel^2 = \frac{c\hbar}{eB_\parallel}. \quad (7)$$

By fitting the theoretical expression (7) to the curves for $\sigma(B_{\parallel})$ (see Fig. 9), we have found the effective thickness of a conducting CuO_2 layer, $d \cong 1.5 \text{ \AA}$. This value yields an estimate for the extent of the electron wave function in the normal direction, and ensures strong carrier confinement ($d < c$). The single crystal NdCeCuO can therefore be regarded as an analog of an ultra-short-period superlattice (1.5 \AA wells / 4.5 \AA barriers).

As the 2D version of weak localization theory is able to describe the behavior of $\sigma(B, T)$ in our sample, the inequality $\tau_{esc} > \tau_{\varphi}$ should be valid for the escape time of an electron from one CuO_2 plane to another. Then we have $\tau_{esc} \geq 5 \times 10^{-11} \text{ s}$. The escape time between adjacent wells in a superlattice can also be estimated from the value of the normal diffusion constant, $\tau_{esc} = c^2/D_{\perp}$. For the parameters of our sample at 300 K, we have [9] $D_{\parallel}/D_{\perp} = 1.7 \times 10^4$ with the in-plane diffusion constant $D_{\parallel} = 1.2 \text{ cm}^2 \text{ s}^{-1}$. Then $\tau_{esc} \cong 5 \times 10^{-11} \text{ s}$ even at room temperature, so $\tau_{esc} > \tau_{\varphi}$ with certainty at low temperatures.

V. CONCLUSION

We have investigated the low-temperature and magnetic field dependence of the normal state in-plane resistivity, ρ_{ab} , in a layered copper oxide single crystal $\text{Nd}_{2-x}\text{Ce}_x\text{CuO}_{4-\delta}$. The material is regarded as an intrinsic two-dimensional conduction system (a collection of 2D conducting CuO_2 planes), and the results are interpreted in terms of the 2D weak localization model. Three indications of 2D weak localization have been displayed: logarithmic temperature dependence of the resistivity, significant negative magnetoresistance for a field normal to the ab -plane, and pronounced magnetoresistance anisotropy (much weaker effect for a parallel configuration). A strong dependence of the magnitude of magnetoresistance on the direction of the magnetic field is the most important experimental test for the two-dimensional character of a conducting system.

In a series of samples with $x = (0.12-0.20)$, we have a full range of disorder parameter values, $k_F\ell = (2-150)$. Estimates of essential microscopic parameters, such as the elastic mean free path ℓ , the inelastic scattering length L_{φ} , and the effective thickness of a conducting layer d , have shown that in accordance with the adopted model, $d \ll \ell$; $L_{\varphi} \ll t$ (t is the geometrical thickness of a sample). Moreover, our estimates show that the thickness of the conducting layer is less than the distance between CuO_2 layers, $d < c$, and this favors carrier confinement within a separate CuO_2 layer. Thus, the NdCeCuO single crystal can be described as a natural superlattice with a confining potential induced both by the specific $pd\sigma$ symmetry of the electron wave function and strong Coulomb correlation effects.

This research was supported by the Russian Program "Current Problems in Condensed Matter Physics" (Grant No.98004) and the Russian Foundation for Basic Research (Grant No.99-02-17343).

-
- [1] E. Dagotto, *Rev. Mod. Phys.* **66**, 763 (1994).
 - [2] N. M. Plakida "High-temperature superconductors", Moscow, International Program of Education (1996).
 - [3] T. Ito, Y. Nakamura, H. Takagi, and S. Uchida, *Physica C* **185-189**, 1267 (1991);
T. Ito, H. Takagi, S. Ishibashi T. Ido and S. Uchida, *Nature* **350**, 596 (1991).
 - [4] S. Uchida, H. Takaji and Y. Tokura, *ISEC-89*, Tokyo, 306 (1989).
 - [5] J. Zaanen, G. A. Sawatsky and J. W. Allen, *Phys. Rev. Lett.* **55**, 418 (1985).
 - [6] H. Takagi, S. Uchida and Y. Tokura, *Phys. Rev. Lett.* **62**, 1197 (1989).
 - [7] S. Massidda, N. Hamada, J. Yu. and A. J. Freeman, *Physica C* **157** 571 (1989).
 - [8] Z. Z. Wang, T. R. Chien, N. R. Ong et al., *Phys. Rev. B* **43** 3020 (1991).
 - [9] A. I. Ponomarev, V. I. Tsidilkovski, K. R. Krylov et al., *Journal of Superconductivity* **9**, 27 (1996).
 - [10] Beom-hoan O and J. T. Markert, *Phys. Rev. B* **47**, 8373 (1993).
 - [11] Y. Hidaka, Y. Tajima, K. Sugiyama et al. *J.Phys. Soc. Jap.* **60**, 1185 (1991).
 - [12] S. J. Hagen, X. Q. Xu, W. Jiang et al., *Phys. Rev. B* **45**, 515 (1992).
 - [13] A. Kussmaul, J. S. Moodera, P. M. Tedrow et al., *Physica C* **177**, 415 (1991).
 - [14] S. Tanda, M. Honma and T. Nakayama, *Phys. Rev. B* **43**, 8725 (1991).
 - [15] A. A. Ivanov, S. G. Galkin, A. V. Kuznetsov et al., *Physica C* **180**, 69 (1991).
 - [16] X. Q. Xu, S. N. Mao, Wu Jiang et al., *Phys. Rev. B* **53**, 871 (1996).
 - [17] A. I. Ponomarev, K. R. Krylov, G. I. Harus et al., *JETP Lett.* **62**, (1995).
 - [18] G. I. Harus, A. N. Ignatenkov, N. K. Lerinman et al., *JETP Lett.* **64**, 444 (1996).
 - [19] Y. X. Jia, J. Z. Liu, M. D. Lan et al., *Phys. Rev. B* **47**, 6043 (1993).

- [20] M. I. Dyakonov, *Sol. St. Commun.* **92**, 711 (1994).
- [21] P. A. Lee and T. V. Ramakrishnan, *Rev. Mod. Phys.* **57**, 287 (1985).
- [22] S. Hikami, A. Larkin and Y. Nagaoka, *Progr. Theor. Phys.* **63**, 707 (1980).
- [23] B. L. Altshuler, A. G. Aronov, A. P. Larkin, D. E. Khmel'nitskii, *JETP* **81**, (1981).
- [24] A. V. Samoilo'v, N.-C. Yeh and C. C. Tsuei, *Phys. Rev. B* **57**, 1206 (1998).
- [25] B. L. Altshuler and A. G. Aronov, *JETP Lett.* **33**, (1981).

Table 1.

x	t , Å	T_c , K	$\rho_0 \times 10^5$, ohm·cm	$\rho_{300 K} \times 10^5$, ohm·cm	$\rho_{300 K}/\rho_0$	$A \times 10^9$, ohm·cm/K ²
0.12	5500	-	-	102	-	-
0.15	5000	20	8.2	42.4	5.2	4.0
0.17	5700	12	8.6	29.6	3.4	2.7
0.18	5000	6.0	6.0	23.5	3.9	2.2
0.20	4000	< 1.3	1.1	10.0	9.1	1.1

Table 2.

x	$n \times 10^{-22}$, cm ⁻³	$k_F \ell$	ℓ , Å	B_{tr} , T	B_{c2}^\perp , T ($T = 1.4$ K)	ξ , Å
0.12	0.2*	2	~ 10	~ 270	-	-
0.15	2.0*	18	~ 30	~ 30	5.5	180
0.18	1.1	25	40	22.5	4.0	200
0.20	1.0	150	240	0.6	2.2	150

* Data from Ref. [4] at $T = 80$ K.

Figures

Fig. 1. Crystal structure of three types of copper oxides (Ref. [4]).

Fig. 2. Phase diagram of $\text{Nd}_{2-x}\text{Ce}_x\text{CuO}_{4-\delta}$. Notation: triangles and circles - data of Ref. [4] (triangles - $T_c = 0$); crosses - our data.

Fig. 3. Temperature dependence of in-plane resistivity for the samples investigated $\text{Nd}_{2-x}\text{Ce}_x\text{CuO}_{4-\delta}$.

Fig. 4. In-plane resistivity ($j \perp B$) of the sample with $x = 0.20$ as a function of magnetic field $B \perp ab$ at two different temperatures. Arrows indicate values of the second critical field. Inset : Hall coefficient ($j \parallel ab; B \perp ab$) as a function of magnetic field at $T = 1.3$ K.

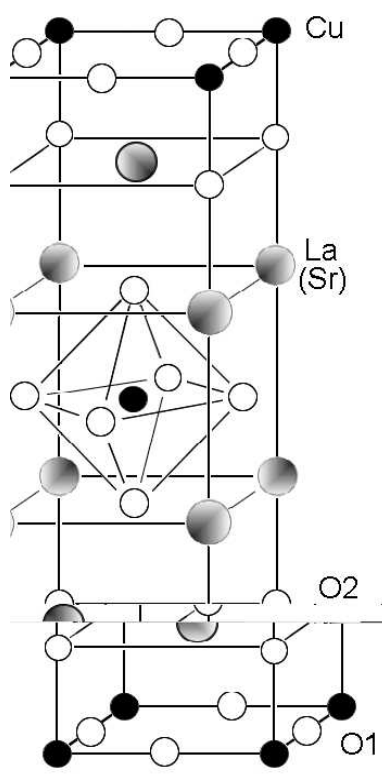
Fig. 5. In-plane resistivity ($j \perp B$) of the sample with $x = 0.18$ as a function of magnetic field $B \perp ab$ at different temperatures. Inset: Hall coefficient ($j \parallel ab; B \perp ab$) as a function of magnetic field at $T = 0.2$ K. The arrow shows the estimate for the second critical field.

Fig. 6. Negative magnetoresistance at $B > B_{c2}$ in the sample with $x = 0.18$. Arrows indicate values of the second critical field B_{c2} at different temperatures.

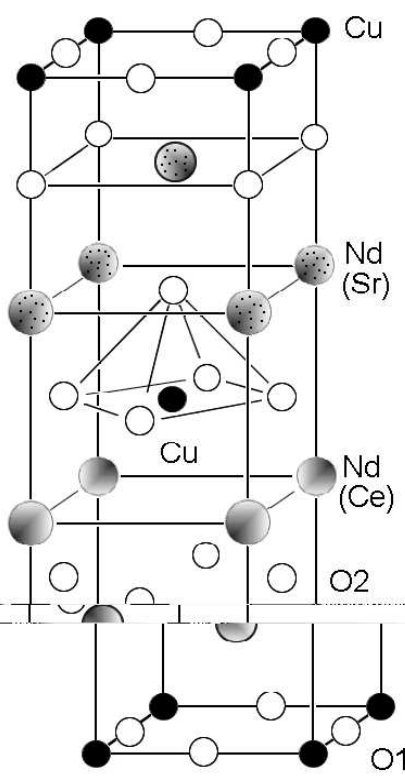
Fig. 7. Fit of the expression (4) to experimental data on the surface conductivity of the sample with $x = 0.18$ at $T = 0.2$ K. Fit parameters of the broken line are: $B_\varphi = 0.1$ T, $\alpha = 6.6$. Inset: Surface conductivity as a function of $\ln B$.

Fig. 8. In-plane resistivity of the sample with $x = 0.18$ as a function of $\ln T$ in different magnetic fields.

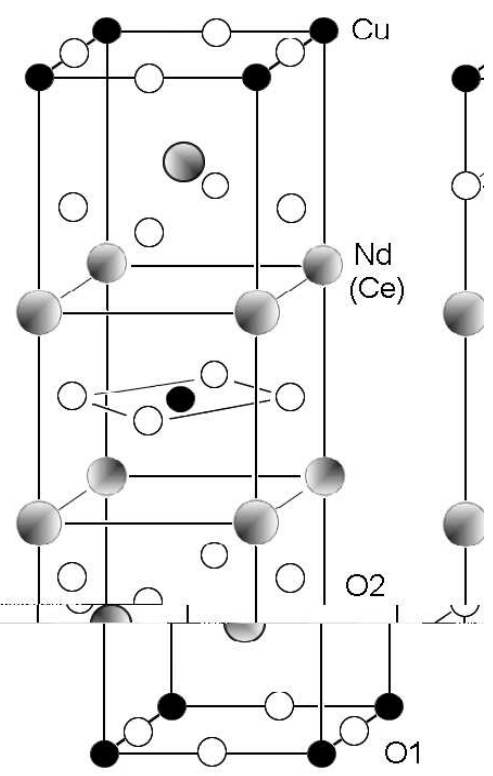
Fig. 9. Surface conductivity of the sample with $x = 0.12$ as a function of magnetic field B_\perp ($B \perp ab$) or B_\parallel ($B \parallel ab$) at different temperatures.



T



T*



T'

